

## ABSTRACT:

Satellite sea-surface salinity (SSS) observations provide a new means for constraining an important state parameter in numerical ocean models. The benefits of assimilating satellite SSS observations include improved model surface density, near-surface convection, and thermohaline circulation. NOAA's Real Time Ocean Forecast System (RTOFS)-Global employs an eddy-resolving 1/12<sup>th</sup>-degree (approximately 9 km horizontal resolution) Hybrid Coordinate Ocean Model (HYCOM). In the current operational configuration, the RTOFS-Global sea-surface salinity is relaxed to PHC3 (Polar Science Center Hydrographic Climatology) climatological SSS fields. Experiments that separately use satellite SSS data and the PHC3 SSS climatology have been conducted to assess the impact of remotely-sensed surface salinity measurements on simulated upper-ocean salinity, temperature, and sea-surface height fields. The first phase of experiments employs a lower-resolution (1/4<sup>th</sup>-degree horizontal resolution) HYCOM model, a potential successor to the Modular Ocean Model as the oceanic component of a future version of NOAA's seasonal-interannual coupled Climate Forecast System (CFS). Results from when using satellite data are compared to results from NOAA's operational configuration, which uses an annual cycle of climatological monthly-mean SSS values. The model's sensitivity to constraining SSS to satellite measurements is explored in terms of relaxation strength and satellite data update interval using monthly-mean and nine-day-running-mean satellite SSS data from the European Space Agency's Soil Moisture – Ocean Salinity (SMOS) mission.

## MODEL:

NOAA's operational Real Time Ocean Forecast System (RTOFS) – Global uses the Hybrid Coordinate Ocean Model (HYCOM; Bleck, 2002) for its computational core.

- Eddy resolving: 1/12<sup>th</sup>-degree horizontal resolution (~ 9 km)
- 32 vertical layers with the KPP mixed-layer formulation
- Coupled to a thermodynamic energy-loan sea-ice model
- Runs daily to produce an 8-day forecast (Mehra et al., 2011)
- Operational configuration: surface salinity is relaxed to PHC3 SSS climatological fields**

This study employs a 1/4<sup>th</sup>-degree horizontal resolution HYCOM version, a potential successor to the current oceanic component in a future version of NOAA's seasonal-interannual coupled Climate Forecast System (CFS).

## DATA:

- Forcing**
  - NOAA/NCEP Climate Forecast System Reanalysis (CFSR)
- Salinity**
  - PHC3 SSS climatological fields (Polar Science Center Hydrographic Climatology); **operational configuration**
  - European Space Agency's Soil Moisture – Ocean Salinity (SMOS) mission; SMOS-BEC (Barcelona Expert Centre) Level-3 (gridded) SSS, version 2.0 reprocessing
  - Binned full-polarization data from combined ascending and descending nodes
  - Spatial resolution = 0.25 degrees
  - Data sets:
    - 9-day mean data set
    - Monthly-mean data set

## METHODOLOGY:

The model was initially run using the NCEP Climate Forecast System Reanalysis (CFSR; Saha et al., 2010) monthly-mean climatological forcing (averaged from 1993 to 2009) for 6 years. The heat flux correction was then computed, relative to the Pathfinder SST climatology, using the last two years of the simulation. The model was then spun up for 6 years using the CFSR monthly-mean climatological forcing with the flux correction. Beginning at this point, the model was run with CFSR total (sequential) forcing with the flux correction for the period 1993 to 2012 (control run). In this control run, sea-surface salinity is relaxed to an annual cycle of climatological monthly-mean values of SSS (PHC3 climatology), as is done operationally. Two sets of cases are used to explore the model's sensitivity to constraining SSS to satellite measurements, both in terms of relaxation strength and satellite data update interval. Monthly-mean and 9-day-mean data were used to assess sensitivity to salinity update frequency. Relaxation strength is specified by the modifying the e-folding time ( $30^*H_m/H_s$  days), where  $H_m$  is the mixed-layer depth and  $H_s$  is the depth of surface salinity influence as a fixed ratio to the mixed-layer depth. Greater  $H_s$  depth of influence leads to a shorter e-folding time scale, increasing the constraint on surface salinity by more quickly relaxing surface salinity to the specified SSS reference field.

Case	Relaxation Reference SSS	$H_s$ (relaxation strength)
PHC_CL (control)	PHC monthly-mean climatology	15m
SMOS_MN_15M	SMOS monthly-mean	15m
SMOS_MN_45M	SMOS monthly-mean	45m
SMOS_MN_75M	SMOS monthly-mean	75m
SMOS_MN_105M	SMOS monthly-mean	105m
SMOS_9D_15M	SMOS 9-day mean	15m
SMOS_9D_45M	SMOS 9-day mean	45m
SMOS_9D_75M	SMOS 9-day mean	75m
SMOS_9D_105M	SMOS 9-day mean	105m

The modeled SSS from different cases can be evaluated by the percentage change of root mean square error (RMSE) of SSS. Reduction in RMSE demonstrates improved model performance with respect to matching the reference SSS.

$$\text{Percent RMSE change} = \frac{RMSE_{CaseB} - RMSE_{CaseA}}{RMSE_{Control}} \times 100$$

where:

$$RMSE_{Control} = \sqrt{\frac{1}{n} \sum (SSS_{Control} - SSS_{Observed})^2} \quad RMSE_{CaseA} = \sqrt{\frac{1}{n} \sum (SSS_{CaseA} - SSS_{Observed})^2} \quad RMSE_{CaseB} = \sqrt{\frac{1}{n} \sum (SSS_{CaseB} - SSS_{Observed})^2}$$

## DISCUSSION:

The only salinity observations currently available for assimilation into models are those from Argo floats and surface ships; consequently, coverage and resolution are very sparse. Satellites, for the first time, provide observations suitable for sufficiently constraining SSS. Observed SSS variability (Fig. 1.a) is notably greater than modeled results when using the PHC climatology (control, Fig. 1.b), introducing representation errors, particularly in equatorial regions. The weaker variability (Fig. 1.b) is likely due to the data comprising the SSS climatology, which are strictly *in situ*, with limited spatial and temporal resolution, muting representation of higher frequencies. Increasing the data update frequency (Fig. 2) has only a slight and mixed impact on modeled variability, predominantly increasing variability in tropical regions while generally decreasing variability in the center of ocean basins, with a focused reduction in the far western Pacific, as well as reductions possibly associated with the Benguela, Agulhas, Canary, and Gulf of Mexico Loop Currents. Improved representation of observed SSS variability is achieved through more tightly the model to observed SSS (Figs. 1.c-f), which also significantly and broadly reduces the RMSE of model results, referenced to SMOS observations (Figs. 3.a-d). Increasing data update frequency (Fig. 4) slightly increases the RMSE generally everywhere.

## Impact of Satellite SSS Data (Monthly-mean)

### SSS Standard Deviation

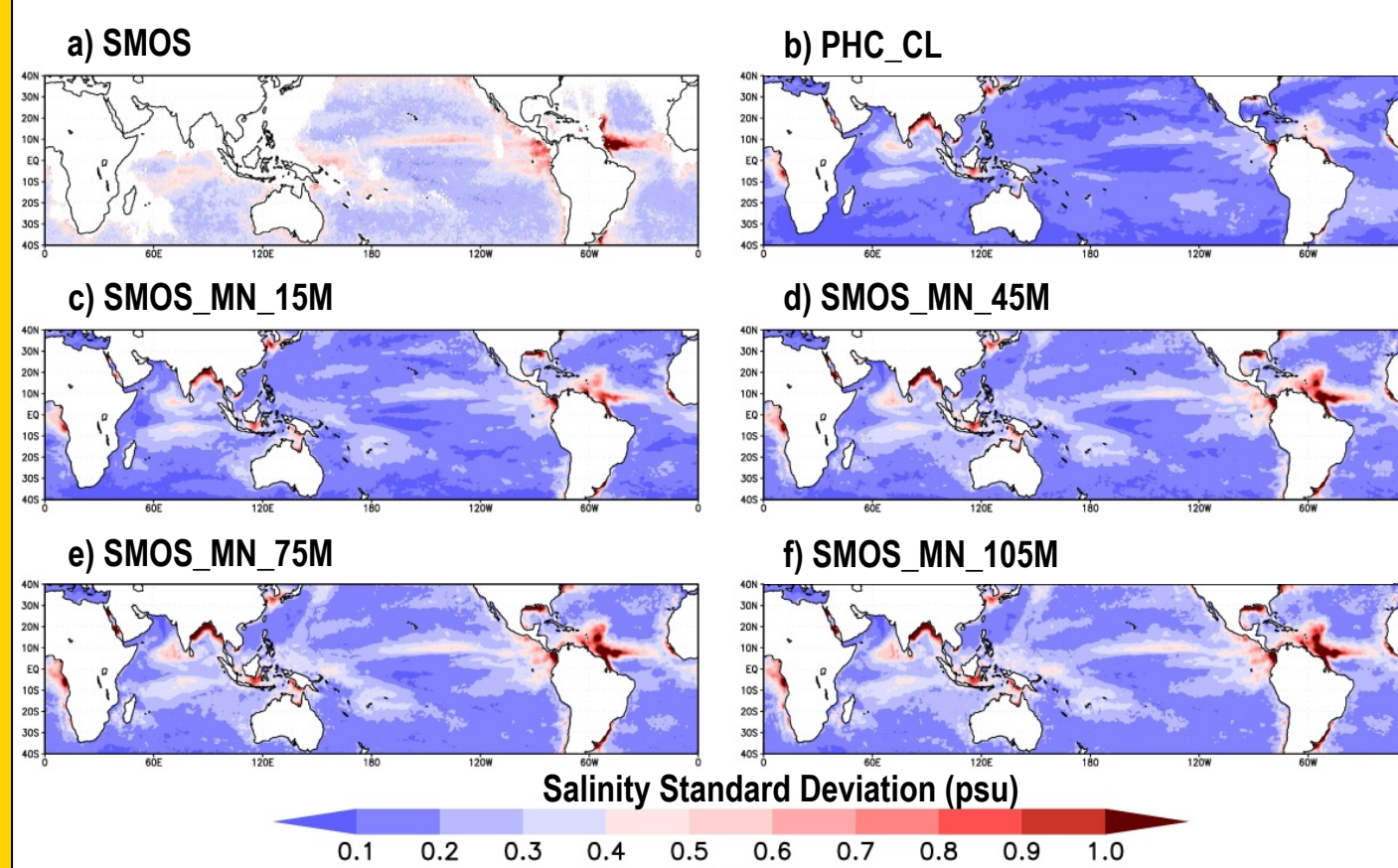


Figure 1. SSS standard deviation: a) SMOS observations, b) PHC climatology, and HYCOM results when using monthly-mean SSS data and increasing constraint to observed SSS, with H<sub>s</sub> = c) 15m, d) 45m, e) 75m, and f) 105m.

## Impact of Near-real-time Data (9-day-mean Minus Monthly-mean)

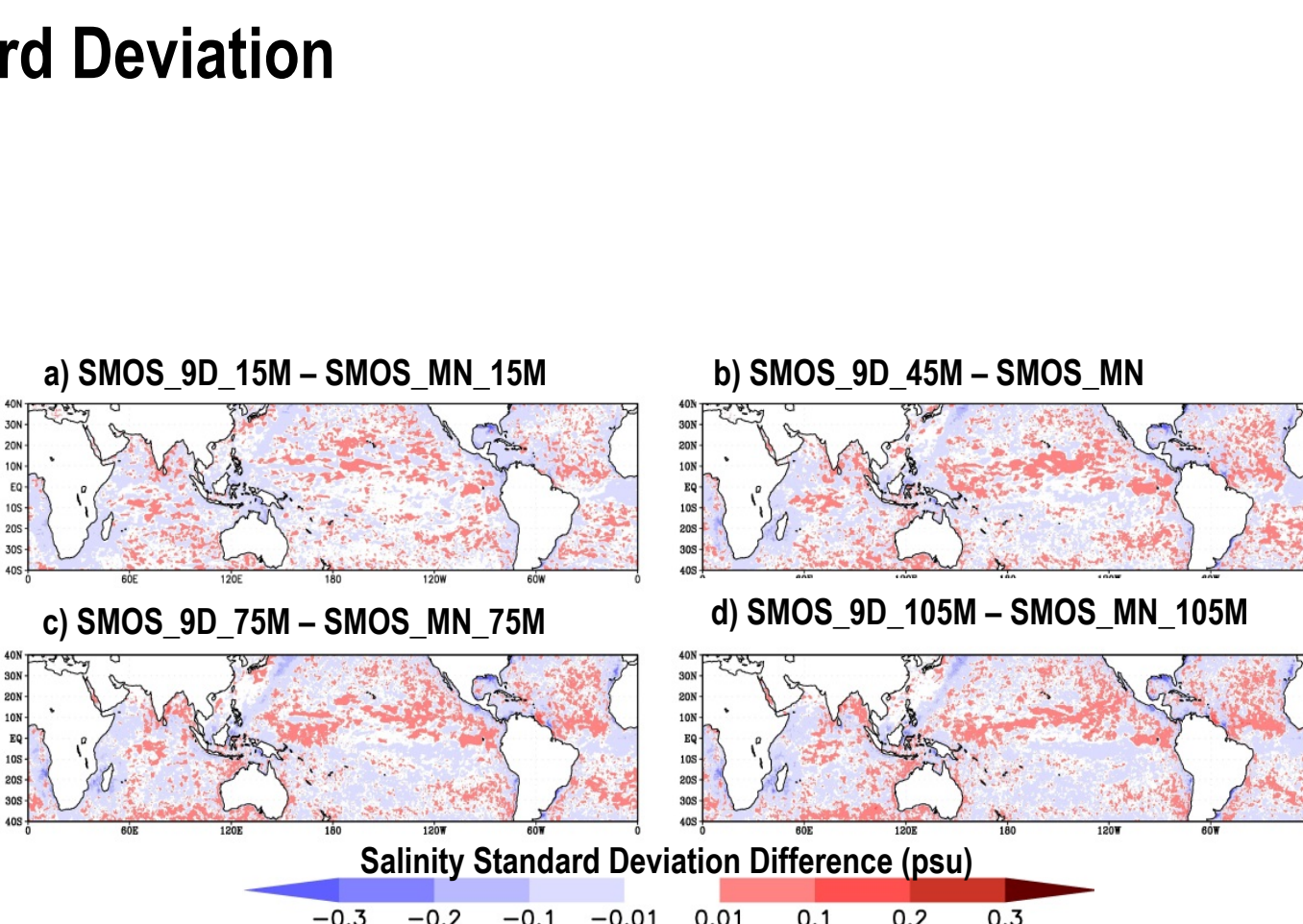


Figure 2. SSS standard deviation difference of HYCOM results when using 9-day-mean SSS data and increasing constraint to observed SSS, with H<sub>s</sub> = a) 15m, b) 45m, c) 75m, and d) 105m.

### Percent Change of SSS RMSE

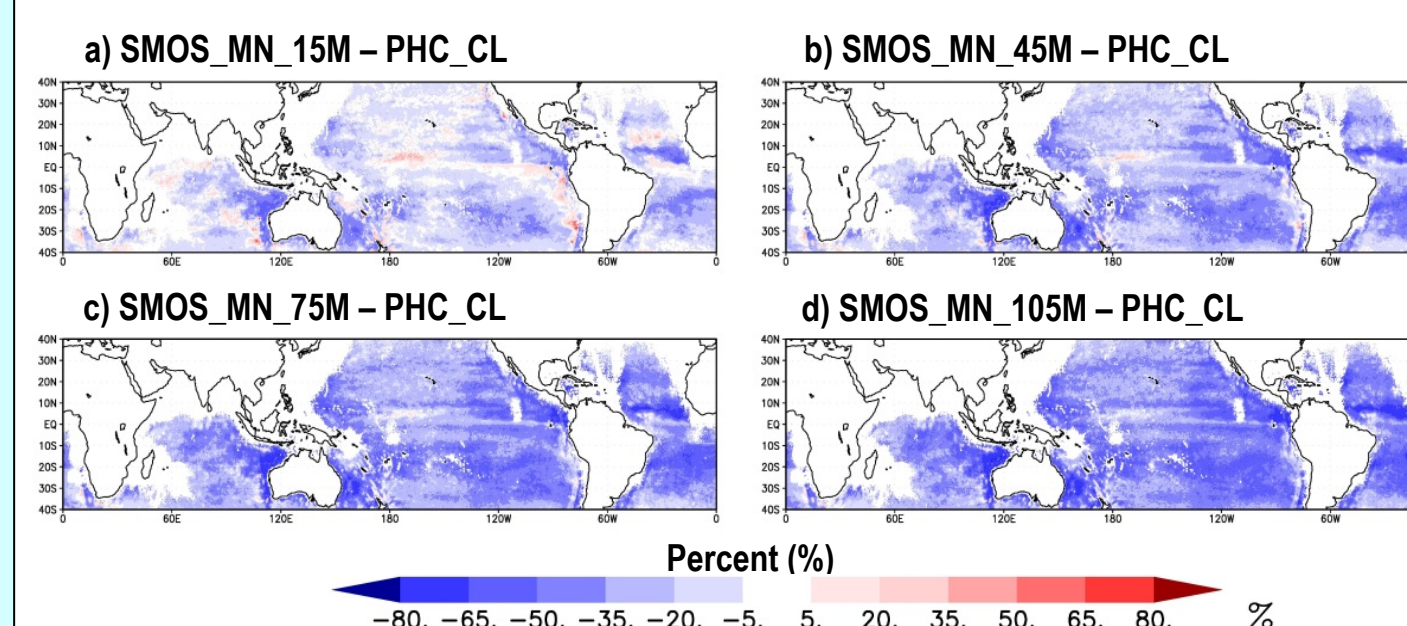


Figure 3. Root mean square error (RMSE) change – SMOS monthly-mean SSS data cases versus control case using PHC SSS climatology, referenced to SMOS observations, with increasing constraint to observed SSS: H<sub>s</sub> = a) 15m, b) 45m, c) 75m, and d) 105m.

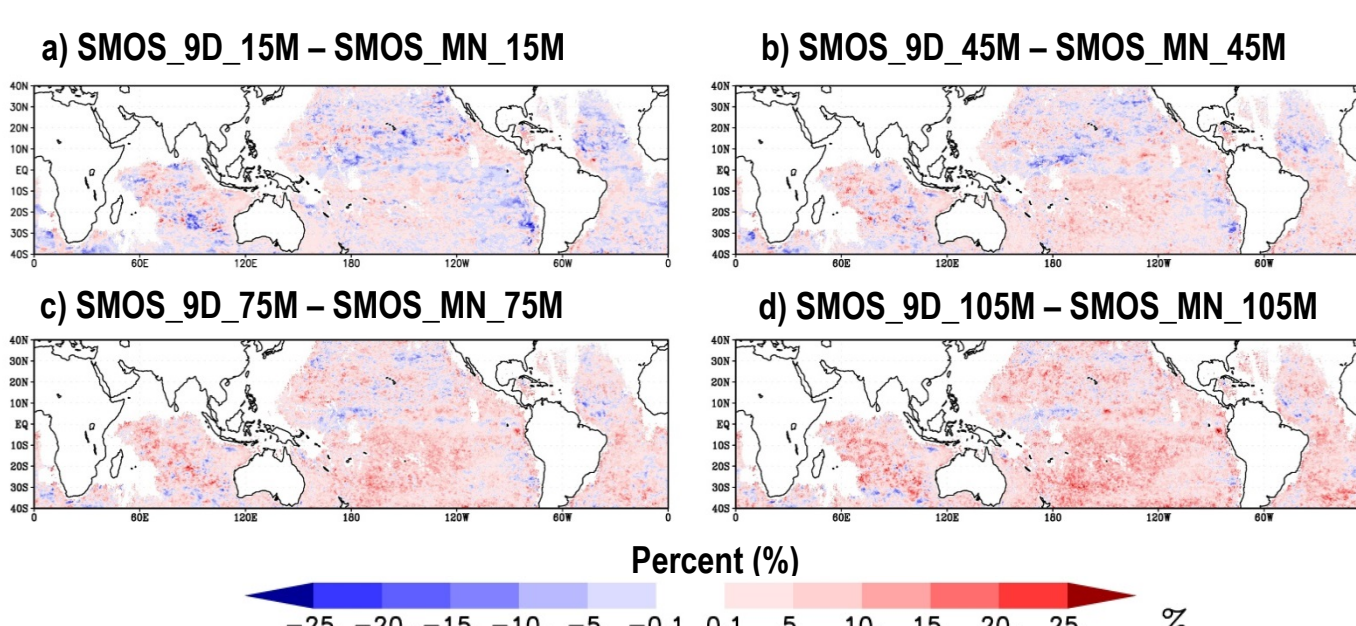


Figure 4. Root mean square error (RMSE) change – SMOS 9-day-mean SSS data cases versus control case using SMOS monthly-mean SSS data, referenced to SMOS observations, with increasing constraint to observed SSS: H<sub>s</sub> = a) 15m, b) 45m, c) 75m, and d) 105m.

## DISCUSSION (cont):

For the equatorial band 5°S - 5°N, more tightly constraining SSS (Fig. 5) produces clear and more intense heating along the thermocline in each of the ocean basins, most notably in the Pacific, with the exception of the far western Atlantic, which experiences stronger cooling. The additional signal from increasing the SSS update rate intensifies the monthly-update heating signal along the thermocline, except in the Atlantic, where the additional signal is the opposite of the monthly signal, cooling along most of the thermocline. At the surface, heating occurs in the eastern Pacific and far western Indian Oceans, while cooling occurs in most of the Atlantic, the western Pacific, and eastern Indian Oceans. Increasing the SSS update rate generally intensifies everywhere the monthly-update signal. This heating pattern for the regions of the Pacific cold tongue and warm pool could have significant impact on ocean-atmosphere coupled modeling. When more tightly constraining model SSS, salinity (Fig. 7) is generally fresher everywhere within the 5°S - 5°N equatorial band, except for the eastern Pacific, not including the core of the cold tongue. Intense freshening occurs in the western Pacific, with narrow bands of comparably intense freshening in the Pacific cold tongue and far western Atlantic regions. The freshening seen in the western Atlantic is potentially associated with better representation of freshwater influx from major South American rivers. The additional signal from increasing the SSS update rate (Fig. 8), increases salinity relatively uniformly nearly everywhere in the equatorial band, with some narrow intensification in the far eastern and far western portions of each basin.

Examining near-surface temporal changes of temperature in the Pacific Niño 3 (5°S-5°N, 150°W-90°W) and Niño 4 (5°S-5°N, 160°E-150°W) regions (Fig. 9), differences are focused at the thermocline, at approximately 150 m depth, intensifying with increasing strength of SSS constraint. The character of these changes are the same in both Niño 3 and Niño 4, with Niño 3 experiencing greater intensity changes. Updating the observed SSS more frequently (Fig. 10) generally produces some additional heating at the thermocline.

Near-surface temporal changes of salinity in the Niño 3 and Niño 4 regions (Fig. 11) reveal that constraining the model to satellite SSS observations appears to have a strength threshold beyond which the results change character and then simply intensify, revealing that a minimum strength constraint exists for representative modeling. Providing more frequent updates on the observed SSS (Fig. 12) produces additional intensification that grows somewhat with tighter constraint, without a change of character. In general, the impacts on salinity are confined to the surface, approximately the top 150 m.

Figures 13 and 14 demonstrate the improvement in the model's representation of sea-surface height anomalies (SSHA), referenced to NESDIS/STAR SSH data (Leuliette, et al., 2004), due to the use of satellite SSS data. In general, incorporating satellite SSS data improves model results, with increasing the update rate intensifying local improvements/departures.

### Mean Temperature (5°S - 5°N) Differences: 2010-2012

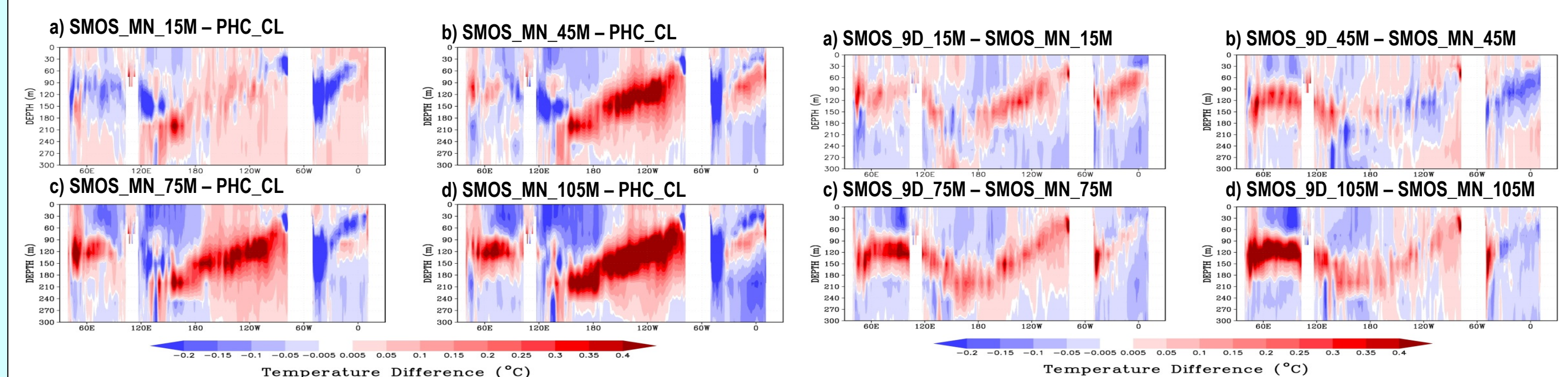


Figure 5. Mean temperature differences for the equatorial band (5°S - 5°N) – SMOS monthly-mean SSS data cases versus control case using PHC SSS climatology, with increasing constraint to observed SSS: H<sub>s</sub> = a) 15m, b) 45m, c) 75m, and d) 105m.

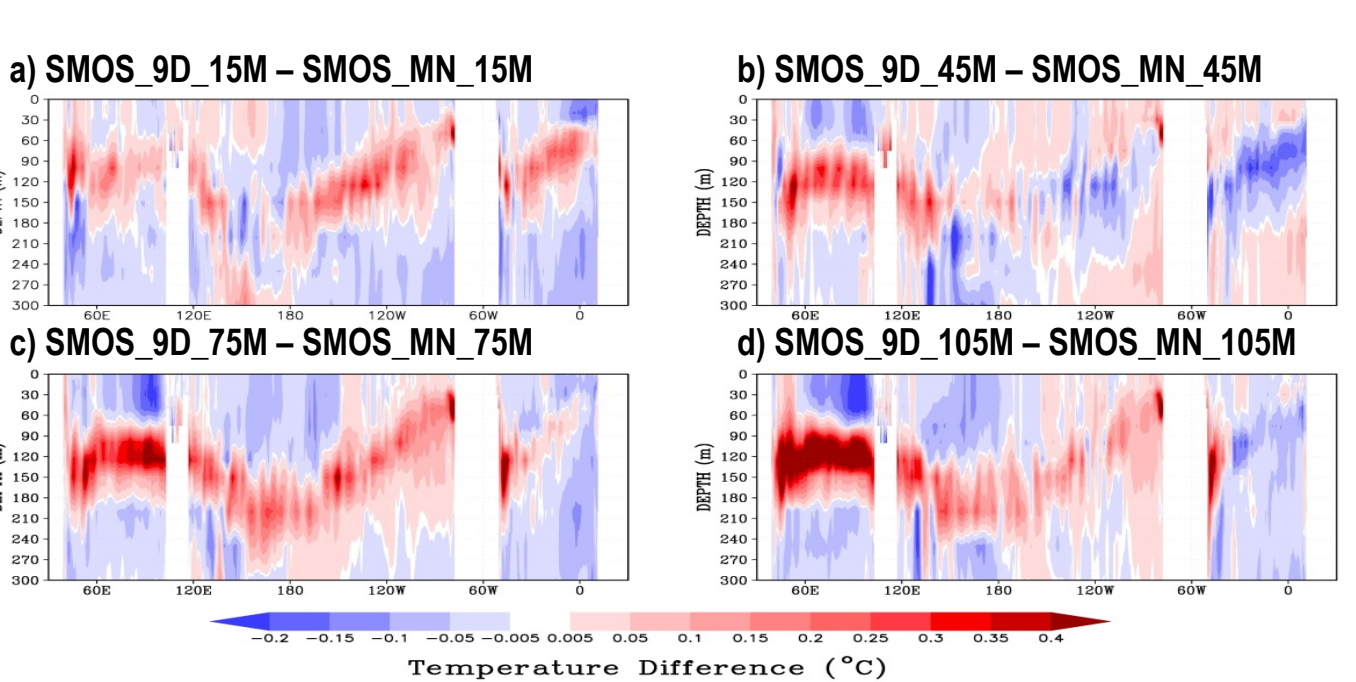


Figure 6. Mean temperature differences for the equatorial band (5°S - 5°N) – SMOS 9-day-mean SSS data cases versus control case using SMOS monthly-mean SSS data, with increasing constraint to observed SSS: H<sub>s</sub> = a) 15m, b) 45m, c) 75m, and d) 105m.

### Mean Salinity (5°S - 5°N) Differences: 2010-2012

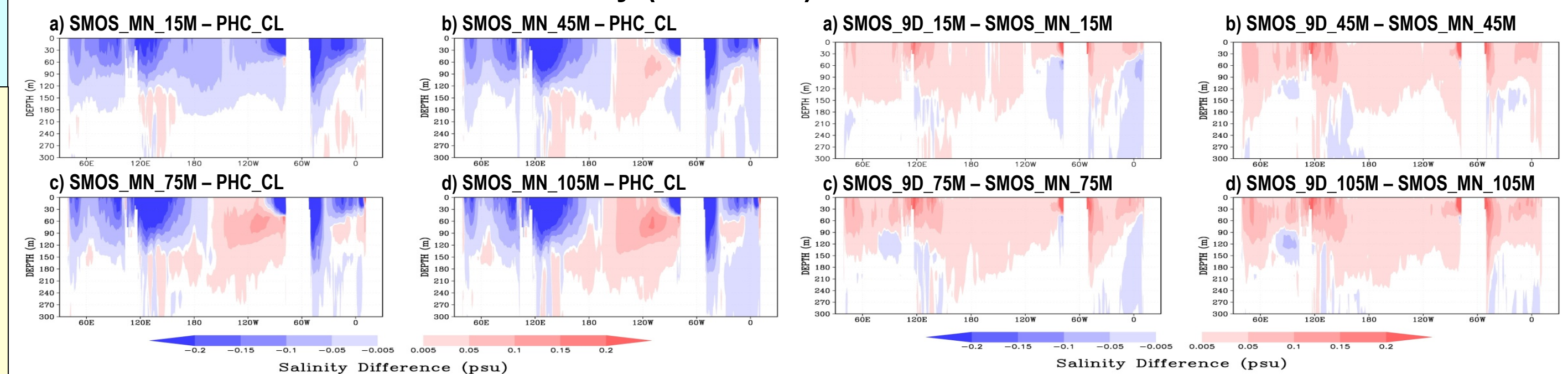


Figure 7. Mean salinity differences for the equatorial band (5°S - 5°N) – SMOS monthly-mean SSS data cases versus control case using PHC SSS climatology, with increasing constraint to observed SSS: H<sub>s</sub> = a) 15m, b) 45m, c) 75m, and d) 105m.

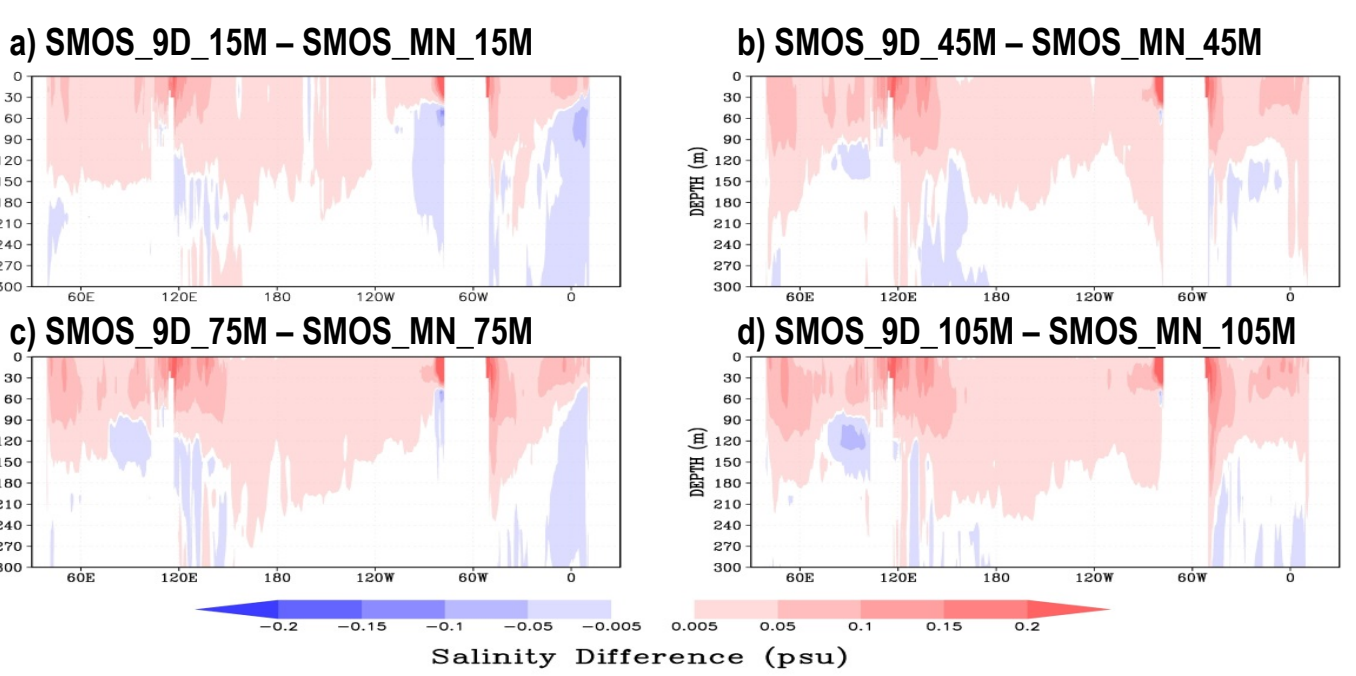


Figure 8. Mean salinity differences for the equatorial band (5°S - 5°N) – SMOS 9-day-mean SSS data cases versus control case using SMOS monthly-mean SSS data, with increasing constraint to observed SSS: H<sub>s</sub> = a) 15m, b) 45m, c) 75m, and d) 105m.

## Impact of Satellite SSS Data (Monthly-mean)

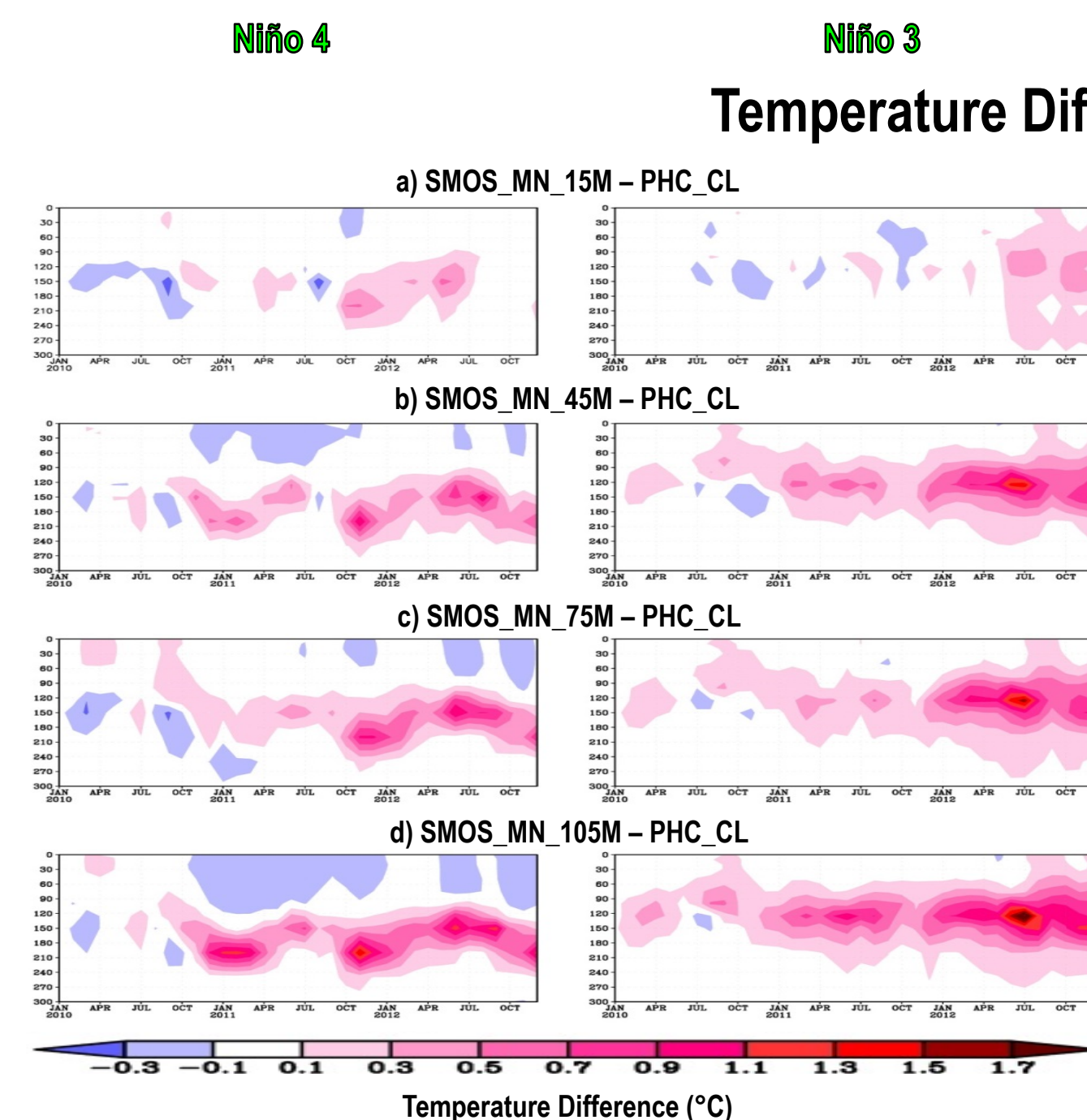


Figure 9. Spatial-mean temperature differences for the top 300 m of equatorial Pacific regions Niño 3 (Eastern) and Niño 4 (Central) – SMOS monthly-mean SSS data cases versus control case using PHC SSS climatology, with increasing constraint to observed SSS: H<sub>s</sub> = a) 15m, b) 45m, c) 75m, and d) 105m.

## Impact of Near-real-time Data (9-day-mean Minus Monthly-mean)

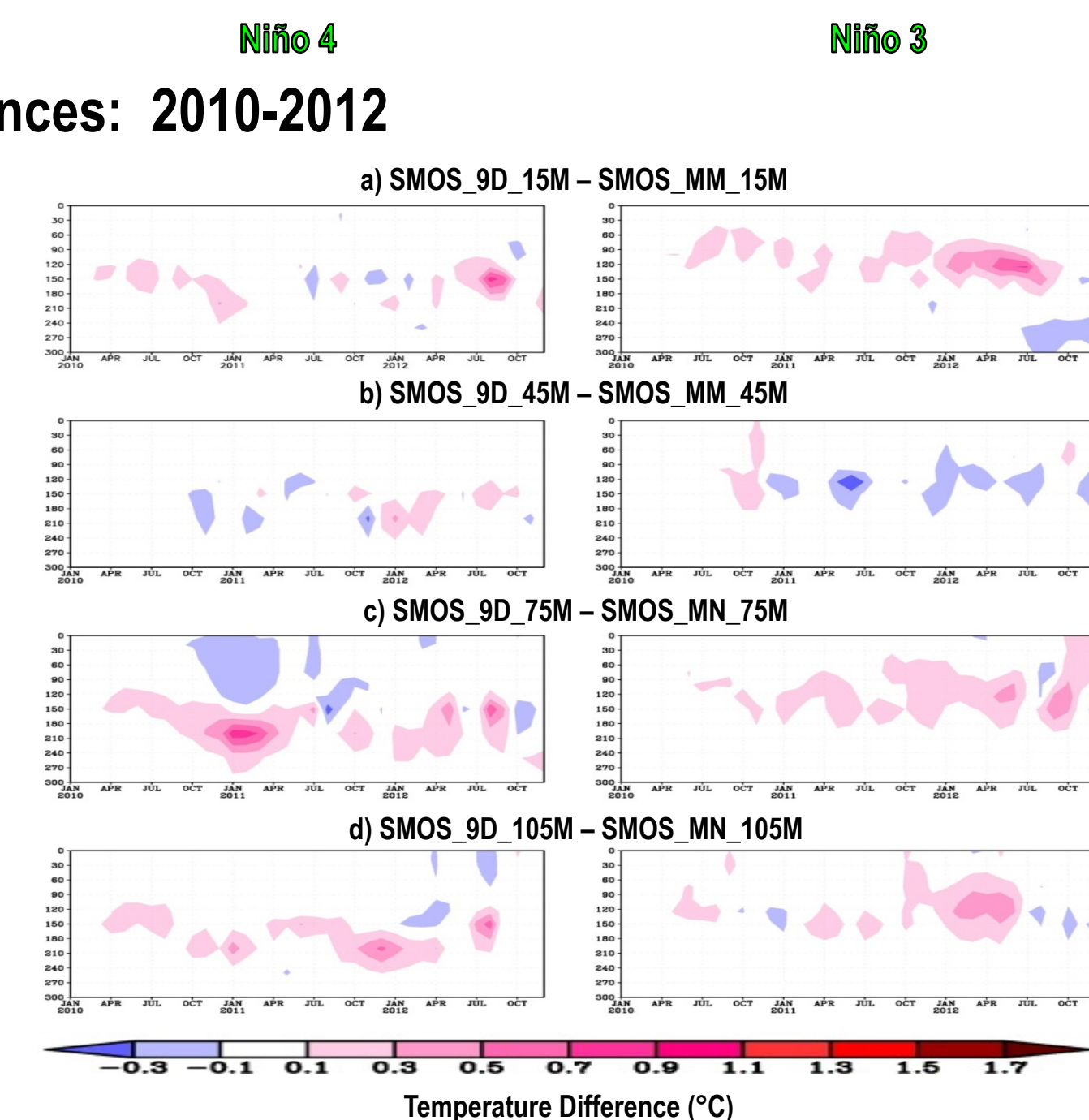


Figure 10. Spatial-mean temperature differences for the top 300 m of equatorial Pacific regions Niño 3 (Eastern) and Niño 4 (Central) – SMOS 9-day-mean SSS data cases versus control case using SMOS monthly-mean SSS data, with increasing constraint to observed SSS: H<sub>s</sub> = a) 15m, b) 45m, c) 75m, and d) 105m.

### Salinity Differences: 2010-2012

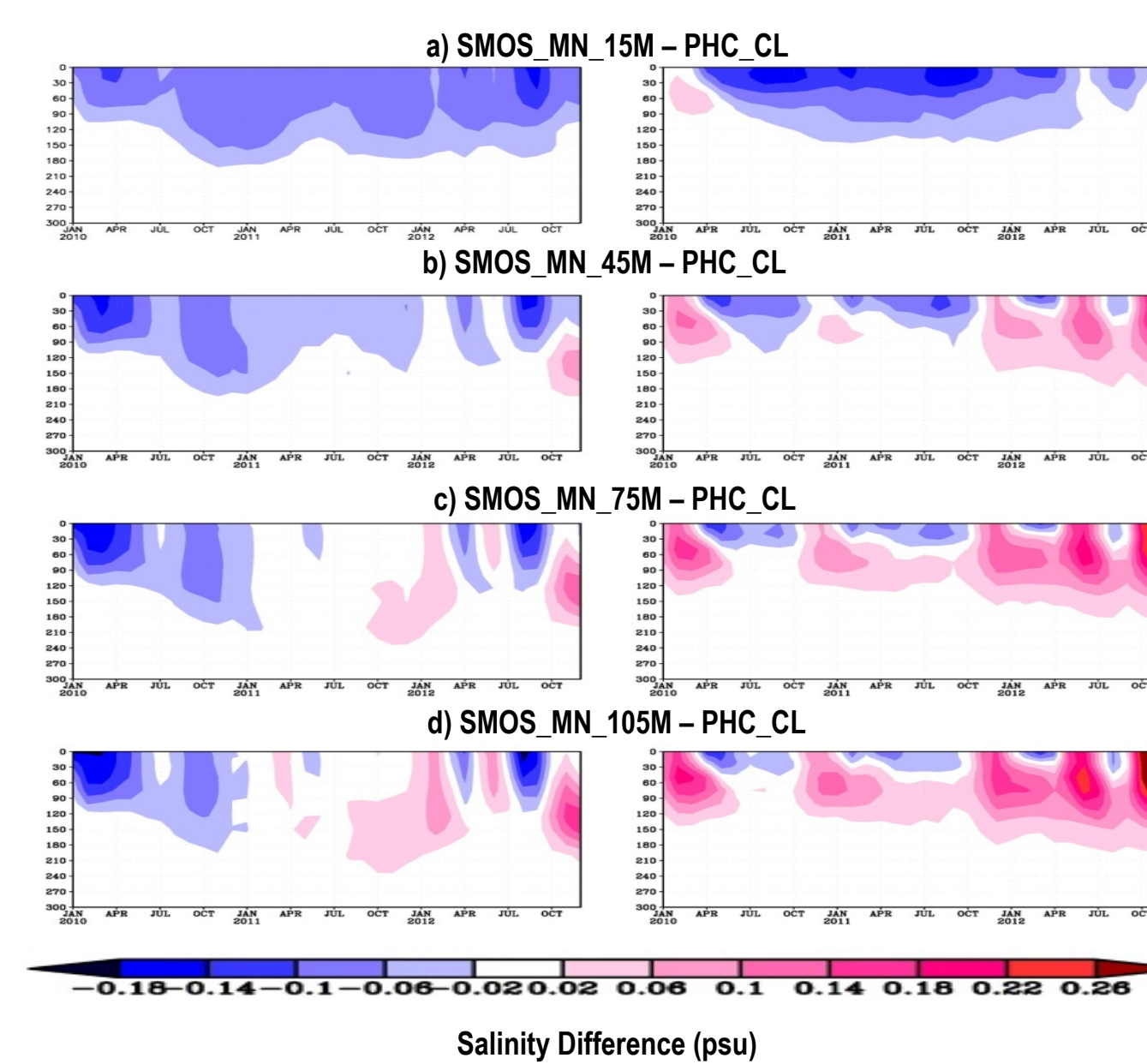


Figure 11. Spatial-mean salinity differences for the top 300 m of equatorial Pacific regions Niño 3 (Eastern) and Niño 4 (Central) – SMOS monthly-mean SSS data cases versus control case using PHC SSS climatology, with increasing constraint to observed SSS: H<sub>s</sub> = a) 15m, b) 45m, c) 75m, and d) 105m.

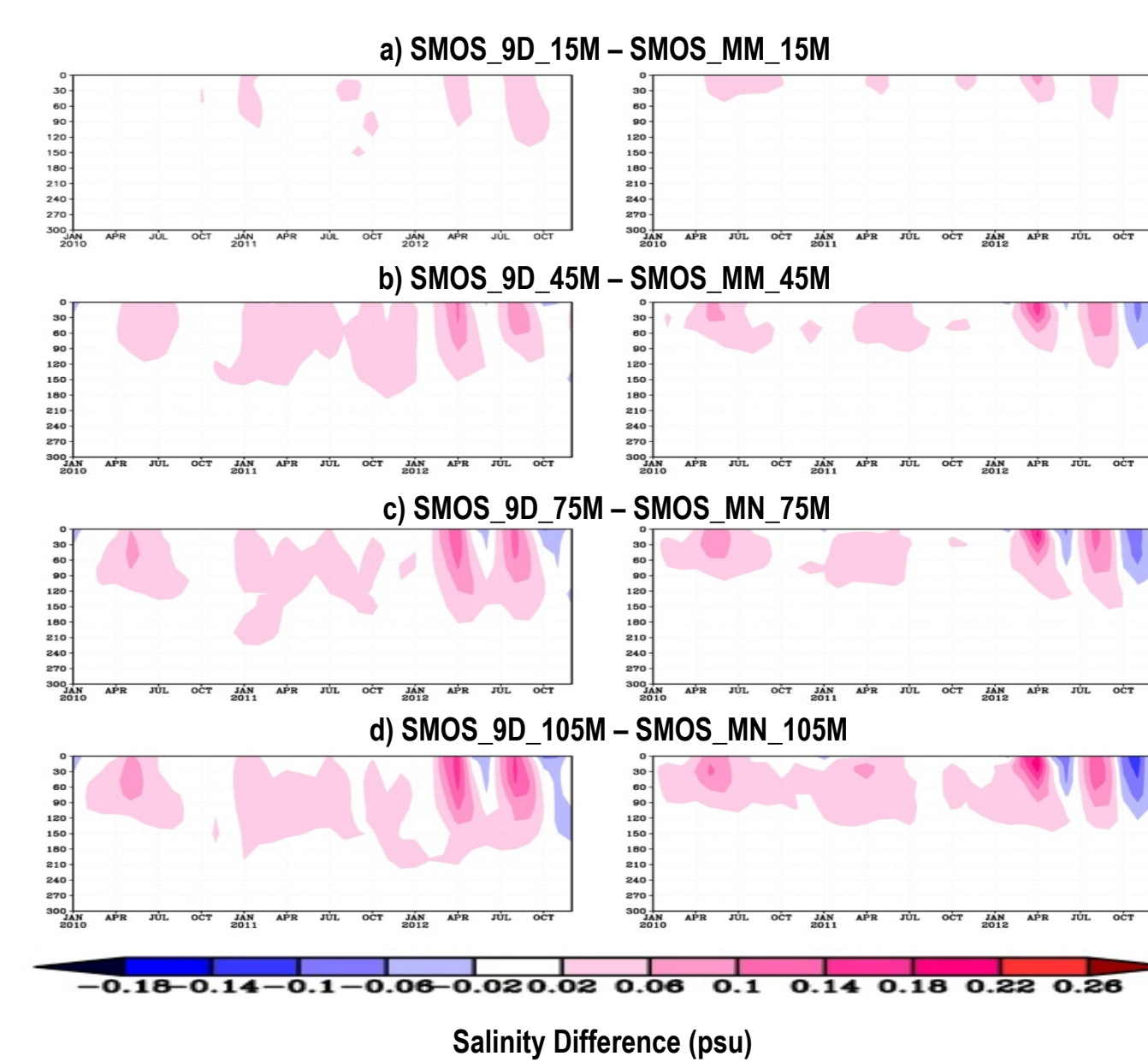


Figure 12. Spatial-mean salinity differences for the top 300 m of equatorial Pacific regions Niño 3 (Eastern) and Niño 4 (Central) – SMOS 9-day-mean SSS data cases versus control case using SMOS monthly-mean SSS data, with increasing constraint to observed SSS: H<sub>s</sub> = a) 15m, b) 45m, c) 75m, and d) 105m.

### Model Sea-surface Height Improvement

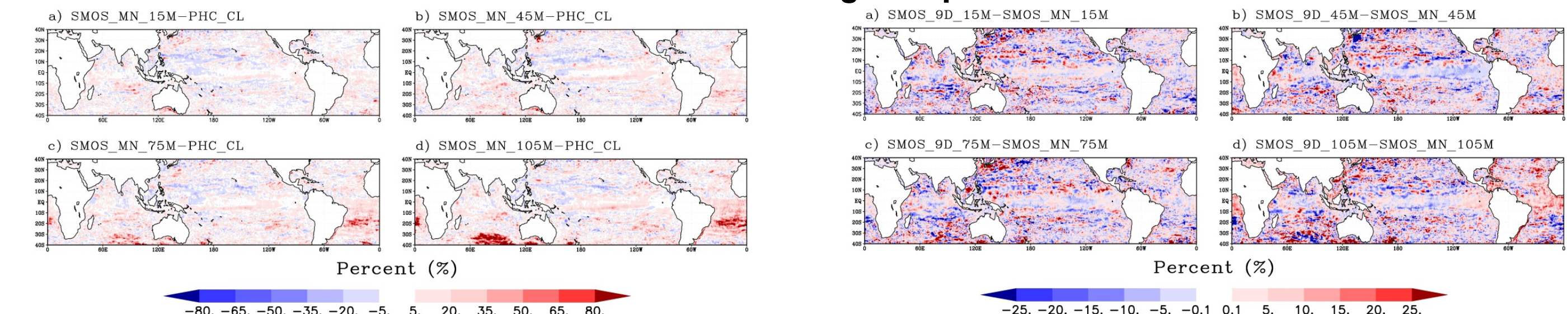


Figure 13. Root mean square error (RMSE) change – SMOS monthly-mean SSS data cases versus control case using PHC SSS climatology, referenced to satellite SSH data, with increasing constraint to observed SSS: H<sub>s</sub> = a) 15m, b) 45m, c) 75m, and d) 105m.

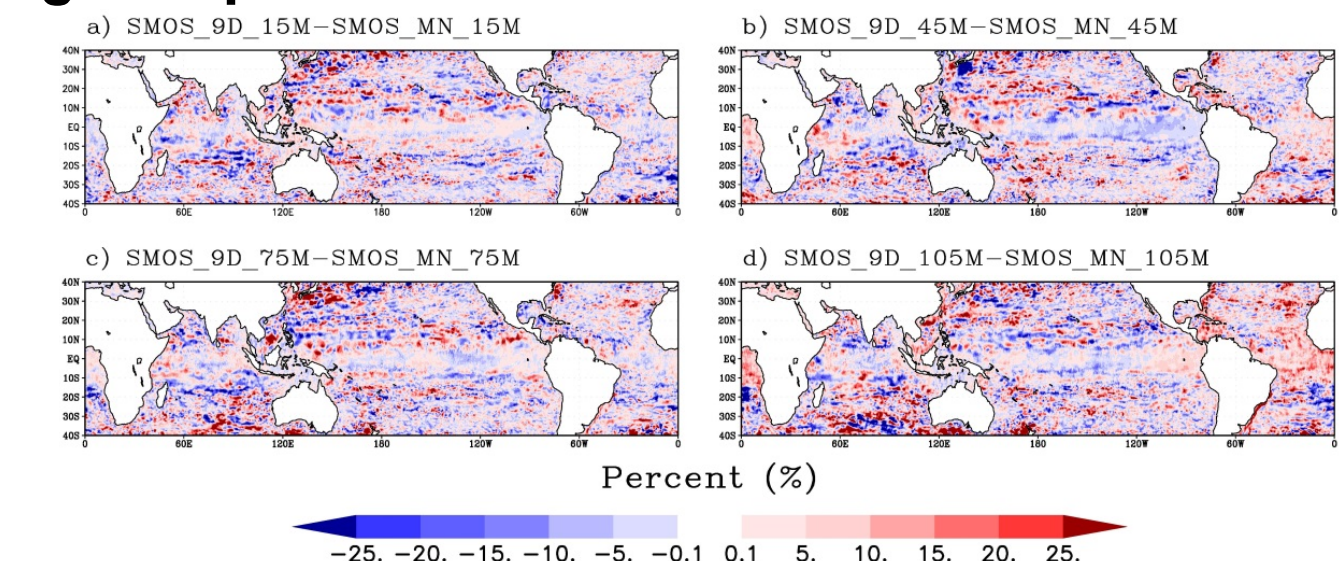


Figure 14. Root mean square error (RMSE) change – SMOS 9-day-mean SSS data cases versus control case using SMOS monthly-mean SSS data, with increasing constraint to observed SSS: H<sub>s</sub> = a) 15m, b) 45m, c) 75m, and d) 105m.

## CONCLUSIONS:

- The use of satellite SSS data for constraining ocean modeling is needed to ensure adequate representation of salinity variability.
- In general, employing satellite SSS observations to constrain modeling, appears to affect the equatorial band (5°S - 5°N) by:
  - Increasing heating at the thermocline, intensifying the heating with greater constraint to observations and updating observations nearer to real time;
  - Producing surface warming in the eastern Pacific, while cooling the surface of the western Pacific, eastern Indian, and most of the Atlantic Oceans;
  - Modifying surface salinity only, with influence confined to approximately the upper 150 m; and
  - Producing surface freshening, everywhere except the east central Pacific, where salinity increases.
- In general, the effect of increasing the frequency of updates for the SSS field referenced for relaxation is to add additional intensification, whether it is heating, cooling, freshening, or salinification.
- In general, incorporating satellite SSS data improves modeled SSHA, with increasing the update rate intensifying local improvements/departures.

In terms of constraining models, models have long had a good initial temperature state, but not a good initial salinity state. While satellite SSS observations improve the situation, the number of *in situ* subsurface observations remains inadequate. Modeling needs a mechanism for constraining subsurface salinity values; consequently, research needs to explore, not only the use of satellite SSS to constrain modeled surface values, but also how to extract/project meaningful values for the upper-ocean.

## References:

- Bleck, R., 2002: *An oceanic general circulation model framed in hybrid isopycnic-cartesian coordinates*, Ocean Modeling, 4, 55-88.
- Leuliette, E.W., RS Nerem, and GT Mitchum, 2004: *Calibration of TOPEX/Poseidon and Jason Altimeter data to construct a continuous record of mean sea level change*, Marine Geodesy 27, no. 1 (2004): 79.
- Mehra A., I. Rivin, H.L. Tolman, T. Spindler and B. Balasubramanian, 2011: *A Real Time Operational Global Ocean Forecast System. Presented at US GODAE Ocean View Workshop on Observing System Evaluation and Inter-comparisons*, Univ. of California Santa Cruz, CA, USA, 13-17 June 2011.
- Saha, S., et al., 2010: *The NCEP Climate Forecast System Reanalysis*, Bull. Amer. Meteor. Soc., 91(8), 1015-1057 (DOI: 10.1175/2010BAMS3001.1).
- Steele, M., R. Morley, and W. Ermold, 2001: *PHC: A global ocean hydrography with a high quality Arctic Ocean*, J. Climate, 14, 2079-2087.
- SMOS-BEC Team, 2015: *SMOS-BEC Ocean and Land Products Description, BEC-SMOS-0001-PD.pdf version 1.4 dated 18 Jun 2015*, <http://www.smos-bec.icm.csic.es>.